energies

MDPI

Article

Energy Conservation in an Office Building Using an Enhanced Blind System Control

Edorta Carrascal-Lekunberri [1,*], Izaskun Garrido [2], Bram van der Heijde [3,4,5], Aitor J. Garrido [2], José María Sala [6] and Lieve Helsen [3,4]

1 Automatic Control Group, Department of Thermal Engineering, University of the Basque Country (UPV/EHU), 48013 Bilbao, Spain
2 Automatic Control Group, Department of Automatic Control and System Engineering, University of the Basque Country (UPV/EHU), 48013 Bilbao, Spain; izaskun.garrido@ehu.eus (I.G.); aitor.garrido@ehu.eus (A.J.G.)
3 EnergyVille, 3600 Genk, Belgium; bram.vanderheijde@kuleuven.be (B.v.d.H.); lieve.helsen@kuleuven.be (L.H.)
4 Simulation of Thermal Systems, Division TME, Department of Mechanical Engineering, KU Leuven, 3001 Leuven, Belgium
5 Flemish Institute for Technological Research (VITO), 2400 Mol, Belgium
6 Department of Thermal Engineering, University of the Basque Country (UPV/EHU), 48013 Bilbao, Spain; josemariapedro.sala@ehu.eus
* Correspondence: edorta.carrascal@ehu.eus; Tel.: +34-656-754-135

Academic Editor: Hossam A. Gabbar (Gaber)
Received: 30 November 2016; Accepted: 1 February 2017; Published: 10 February 2017

Abstract: The two spaces office module is usually considered as a representative case-study to analyse the energetic improvement in office buildings. In this kind of buildings, the use of a model predictive control (MPC) scheme for the climate system control provides energy savings over 15% in comparison to classic control policies. This paper focuses on the influence of solar radiation on the climate control of the office module under Belgian weather conditions. Considering MPC as main climate control, it proposes a novel distributed enhanced control for the blind system (BS) that takes into account part of the predictive information of the MPC. In addition to the savings that are usually achieved by MPC, it adds a potential 15% improvement in global energy use with respect to the usually proposed BS hysteresis control. Moreover, from the simulation results it can be concluded that the thermal comfort is also improved. The proposed BS scheme increases the energy use ratio between the thermally activated building system (TABS) and air-handling unit (AHU); therefore increasing the use of TABS and allowing economic savings, due to the use of more cost-effective thermal equipment.

Keywords: model predictive control (MPC); enhanced blind system control (BSC); thermally activated building system (TABS); two office model; energy savings; solar irradiation; thermal comfort

1. Introduction

The implementation of energy saving measures in the building sector is nowadays key in energy development policies supported by the European Union to reduce both its energetic dependence and the emissions of greenhouse gases. Simultaneously, thermal comfort requirements must still be met. On the path towards energy efficiency, the use of an appropriate control for heating, ventilation and air-conditioning (HVAC) systems can be as important as the use of improved construction materials and the thermal insulation of the building envelope [1].

Being a low exergy thermal system, TABS takes advantage of the high thermal inertia of the building structure and becomes an adequate choice to achieve significant economic and energetic savings when used under an appropriate HVAC control as model predictive control, MPC.

Many authors have studied the behaviour and modelling of a specific TABS, Concrete Core Activation (CCA), where the concrete floor or ceiling is thermally activated. Most importantly, the heat transfer model by Koschenz and Lehmann [2], the RC equivalent network model by Weber et al. [3] and its validation in the frequency and time domain by Weber and Jóhannesson [4] deserve to be mentioned here. The advantage of a high thermal inertia for efficient heating and cooling requires an adequate control strategy in order to avoid overheating, undercooling or destroying useful cooling or heating power by compensating it before it has reached the adjacent zone as described by Sourbron et al. [5]. Therefore, usually MPC is proposed because it explicitly considers these slower system dynamics as explained by Gwerder et al. [6].

The chosen HVAC control strategy for buildings influences the amount of energy needed to meet comfort requirements. Although On-Off switch and rule-based control (RBC) are widely used control schemes in office buildings, the need to improve the energetic and economic efficiency of the HVAC systems calls for more advanced controls such as the genetic algorithm used by Yu and Nam [7]. The development of schemes as the classical proportional integral (PI) [8], fuzzy logic based methods [9], artificial neural networks (ANN) [10] or fuzzy and MPC integration [11] allow for the reduction of the energy use while maintaining the required thermal comfort.

In the last years the domain where MPC is implemented has expanded, from the first papers about its applications in the chemical field by Richalet et al. [12] to a wide spectre of studies and applications as the plasma control simulations of Garrido et al. [13,14], the trajectory generation of unmanned aerial vehicles as describe Singh and Fuller in [15], the management of the energy for electric vehicles provided by Ji et al. [16] or even in the treatment of diabetes as described in [17]. In the building sector, the literature shows multiple studies and implementation cases such as the ones associated to the OptiControl project collected in [18] by Gyalistras et al. and in [19] by Gwerder et al., those related to the work of Picard et al. [20] and Antonov [21] or the recent study of Killian and Kozek [22] about the important aspects associated with the use of MPC in energy efficient buildings. Focused on energy saving policies, some of those studies show reductions in the energy use of about 15% or even higher. As an example, the study of De Coninck and Helsen [23] suggests an energy cost reduction of 30% for an office building in Brussels while Široký et al. [24] studied the behaviour of different buildings getting potential energy saving ranging from 15% to 28%. The studies in Australia of West et al. [25] provide energy savings of 19% and 32%. Although the MPC in building sector is usually applied to office blocks, there are also successful studies on other buildings typologies, namely residential buildings, as the gathered by Carrascal et al. in [26] where the study of MPC in a low construction quality building provides potential energy savings over 15%. The use of MPC for scheduling the energy use in residential buildings is studied by Chen et al. in [27]. Meanwhile Patteeuw and Helsen [28] focused on the reduction of CO_2 emissions of residential heating systems by using MPC. Therefore, it is nowadays possible to consider MPC as an appropriate control for building climate applications.

The usage of an MPC to develop the control policies of HVAC systems exploits the knowledge of the predicted values of variables like meteorological disturbances or the heat gains associated to the activity in the building. Moreover, it can use information about the variation of the comfort conditions over time, the use of different climate equipment or the changes in energy rates. The control guaranties thermal comfort with a minimum control objective namely energy use. Therefore, the MPC is an improved control option provided that the predicted disturbances are close to the actual disturbances and it has a correct model of the building.

The main challenge MPC has to face towards its successful implementation is the development of an adequate model for the building under study. As the control action is calculated for the prediction horizon, the development of an accurate model of the building is critical to obtain an appropriate response. Good predictions for meteorological variables and use-patterns are also necessary in order to get an adequate response of the system and to maintain the desired comfort conditions. The difference between the modelled and the real behaviour of the building implies an error in control action. This is usually smoothed by using a state estimation filter, namely a Kalman filter [29].

The effect of the difference between predicted and real disturbances also decreases when a filter is applied. Maasoumy et al. [30] discuss the building model uncertainty under the MPC, Zhang et al. [31] discourses about the treatment of uncertainty in weather and occupancy predictions.

Solar radiation is one of the crucial factors regarding the comfort quality of a building. Its incidence on the façade causes the wall temperature to increase, which in turn influences the heat exchange with the interior. Incident radiation through the windows, after reflection and absorption in the glass layers, strikes the indoors walls, floor and furniture, and then propagates to the indoor environment. An appropriate use of this radiation will reduce the power consumption in winter, but it must be avoided in summer to eliminate overheating.

Previous studies have considered a hysteresis control for the blind system (BS) as the one of Sturzenegger et al. [32], presenting the results of the OptiControl project or Sourbron's PhD [33] where the office model used for this study is described. The study of Le et al. [34] about the influence of the BS in the energetic expenses of a building proposes at first stance a hybrid MPC in which the BSC, integrated in the MPC, operates in four discrete positions. A second part of the study proposes a controller by learning from the optimal controller behaviour using a support vector machine. The work of Lawal [35] also studies the integration of the BS in the MPC as a hybrid combination of continuous actions for the heating-cooling system and three discrete positions for the BS based on indoor temperature. The work of Dussault et al. [36] provides a comparison between different control algorithms for smart windows.

As novel scientific contribution, this paper proposes the use of a simple but improved blind system control (BSC), decoupled from the MPC, that enhances the energy savings of the HVAC system regulating the solar radiation through the windows. This paper studies the energetic behaviour of an office module under the influence of the weather conditions of a typical Belgian meteorological year in Ukkel, Brussels region according to TMY3 data. An MPC controls the main action of the HVAC system to maintain thermal comfort conditions. The noticeable influence that solar radiation has on the comfort parameters motivates the detachment of the windows' BS from the main MPC. The study proposes an enhanced control that couples the benefits of the predictive information with the simplicity associated to a BS-dedicated control.

The rest of this paper is organized as follows: the paper describes the elements of the office module used for the study in Section 2. Then, Section 3 characterizes the model of the module and the control schemes used for the HVAC system and the novel BS. It also describes the conditions of the study performed. The results will show the benefits of the proposed BSC in Section 4. Finally, the authors will present their conclusions based on the obtained results.

2. Study of the System: Building, Office Zones and Climate System

The design of the proposed office block allows creating a module that once modelled will represent the thermal behaviour of the building using a simple, repetitive structure. The building is north-south oriented and the module is composed of three spaces, two office zones and a corridor for separation and access. Each office zone is 12 m^2 and the corridor section is 4.32 m^2 leading to the total heated volume 96.3 m^3. Figure 1 shows a scheme of the module with a representation of the HVAC system and disturbances that affect it.

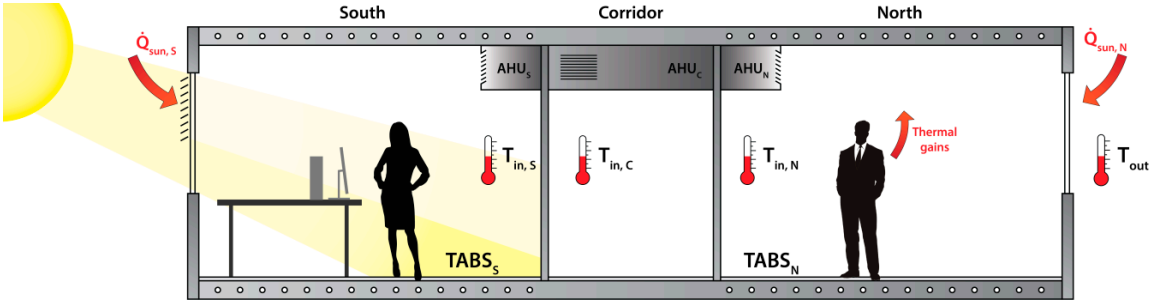

Figure 1. Representation of the modelled two office zones and corridor module.

The model considers the walls between modules to be adiabatic. This follows from the assumption that the temperature of adjacent modules remains the same and the heat flux between them can be neglected. The thermal capacity of the indoor volumes, office zones and corridor, is the combination of the thermal capacity values of the air, the furniture and one of the separating walls. TABS in north and south office zones and air-handling unit (AHU) in office zones and corridor compose the HVAC system. Three main disturbances affect the system: outdoor temperature, solar radiation and internal thermal gains. Outdoor temperature and solar radiation values, as already mentioned, are obtained from a typical meteorological year in Ukkel.

The module model was designed using the IDEAS library (OpenIDEAS Modelica model environment for Integrated District Energy Assessment Simulations (IDEAS), source code available on GitHub (https://github.com/open-ideas/IDEAS)) [37] for Modelica [38], which allows the creation of the model specifying the construction materials, the heating systems action and the disturbances in the module in a similar way as TRNSYS (Thermal Energy System Specialists, LLC, Madison, WI, USA) or EnergyPlus (U.S. Department of Energy, Washington, DC, USA). This kind of representation allows the design of model dynamics close to the real behaviour. Table 1 shows a summary of the characteristic values of the façade of the module used in the model design. Used materials can be said to be considered of high quality. Table 2 presents the characteristics of the module. These values were defined in [33].

Table 1. Technical characteristics of wall layouts and windows.

Wall	***d* (m)**	***U* (W/m^2·K)**
Outer wall	Plaster-Concrete block-Mineral wool-Brick 0.01-0.14-0.1-0.09	0.41
Internal wall	Gypsum board-Mineral wool-Gypsum board 0.012-0.05-0.012	0.79
Floor/Ceiling	Floor tiles-Air layer-Screed-Reinforced concrete with CCA-Plaster 0.04-0.41-0.05-0.2-0.01	1.38
Suspended ceiling	Ceiling tiles-Air layer-Reinforced concrete-Screed-Air layer-Floor tiles 0.01-0.2-0.2-0.05-0.41-0.04	1.11
Window	***U* (W/m^2·K)**	***g* -value**
Window glass	1.10	0.40
Window frame (15%)	2.00	-
Window total	1.29	0.36
Solar shading	-	0.25

Table 2. Module characteristics.

Two Zone Building Parameters	Unit	Value
Area of the South or North zone	m^2	12
Area of the corridor	m^2	4.32
Heated volume	m^3	96.3
Heated area	m^2	28.3
Transmission area	m^2	8.6
U-value external wall	$W/(m^2 \cdot K)$	0.41
U-value total façade	$W/(m^2 \cdot K)$	0.85
Percentage of glazing	%	50

Table 3 describes the internal gains associated to the activity in a standard office and other internal gains. These values are described in ASHRAE Fundamentals [39] for an occupancy of one person/10 m^2 [40], being one of the three disturbances that actuates in the office model. Other operative parameters are also represented. Office hours are considered from 08:00 to 18:00; rest of the time the office is considered unoccupied. In order to describe the internal gains derived from the office use, people occupancy and office appliance use are considered to be from 08:00 to 12:00 and from 13:00 to 18:00. If during office hours no people are present, ventilation and infiltration losses are not compensated by internal heat gains and as a consequence the indoor temperature decreases, as discussed by Reynders [41].

Table 3. Operative parameters of the office module.

Parameter	Value
Occupancy rate	1 person per 10 m^2
Sensible heat gains from people	7.5 W/m^2
Latent heat gains from people	5.5 W/m^2
Appliances heat gains	7.8 W/m^2
Lighting heat gains	7.5 W/m^2
Zone thermal capacitance	5 times the air thermal capacitance.
Convective heat transfer values of floor and ceiling	correlations of Awbi and Hatton [42]
Radiative heat transfer coefficient	5.6 W/m^2
Infiltration rate	0.05 ACH during AHU-operation, 0.2 ACH outside those hours
Ventilation rate	36 m^3/h pers (EN15251 [40] [Class II])

The core purpose of this research is the control of the BS for the windows of the office zones. The main MPC does not integrate this control so as to favour modularity and simplicity of the system. The BS has a hole pattern, which allows all solar radiation to pass when it is open and only 25% when it is closed. Figure 2 shows a representation of this effect.

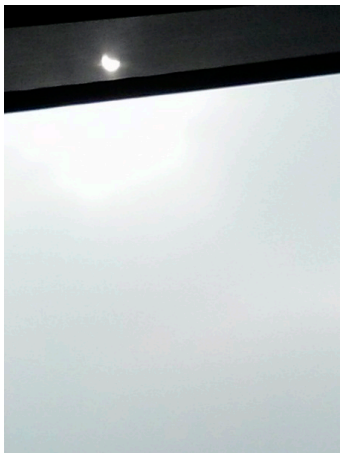

Figure 2. Blind system opacity effect during solar eclipse of 20 March of 2015 in Leuven, Belgium.

The windows are three-layer glass with a global g-value of 0.36, as mentioned in Table 1. The design of the building HVAC system provides the module with two different climate systems:

- Thermally Activated Building System (TABS) is the main option for heating and cooling operations in the building. In order to take advantage of the thermal inertia of the building structure, water pipes are embedded in the concrete, which stores and provides the energy for climate control to the office zones via convection and radiation. Considering the typical heat pump and direct cooling configurations, Sourbron defines in [33] the maximum heating values between 79 and 86 W/m^2 for heating and between 42 and 65 W/m^2 for cooling. The model supposes a power of 50 W/m^2 for both heating and cooling, which provides 600 W power for one office zone. The MPC prioritizes its use by minimizing energy use.
- An auxiliary Air–Handling Unit (AHU), necessary for ventilation and air conditioning, fulfils additional power request. The system adjusts the indoor temperature when the TABS is not able to provide enough heating or cooling power or its response is not quick enough to maintain the comfort conditions. The AHU can contribute with an additional 850 W for heating and cooling in each office zone and 360 W in the corridor.

By simulating the dynamic behaviour of the system under the effect of TABS only for a constant outside temperature and no solar radiation nor internal gains it is possible to calculate the time constant (τ) of the TABS in the office zones. Using the expression:

$$f(\tau) = 0.632(T_{max} - T_{init}) + T_{init} \quad (1)$$

where T_{max} is the temperature at stationary state and T_{init} is the temperature at the beginning of the simulation, The value obtained for τ is about six days.

3. Model and Control Design

3.1. Model

3.1.1. Model Development and Linearization

The model implemented within the MPC consists of three zones: two office zones and a corridor. This is a standard study distribution as bibliography shows [43–46]. The climate control provides an individual regulation of the temperature of each room. As described in Section 2, the Modelica model characterises the module using the specifications of Tables 1–3. The linearization of the model described by Picard et al. in [47] provides a 50 states state-space model that describes the system in matrix notation using a RC representation. These temperature states characterize the system with the temperatures of the office zones and corridor as the control objective. The other states are assigned to the TABS, the wall between office zones and corridor and the temperature of the external façades and windows. The independent treatment of both office zones and the corridor results in a relatively high number of 50 states. In particular, four states characterize the behaviour of each TABS defining the temperature of the concrete and its covering. The façade and the inner partition walls are determined by four further states in each room. No capacity has been considered for windows, whose behaviour is defined by their thermal resistance and g factor. As described by Picard et al. [47], the non-linearity of the transmittance of solar radiation under varying incidence angles is treated as an input to the linearized model. The walls between different office modules and TABS embedded into the floor and ceiling are assumed adiabatic. The model also includes the action of the HVAC system, TABS and AHU, as well as the influence of external perturbations like the weather, the human activity and the use of office devices. The continuous state-space model of 50 states that represents the dynamics of the office module is described in Equation (2). The implementation of the MPC requires a discrete state-space representation of the model that will use a fifteen minutes time step, Ts. The discretization and linearization of the system around the operation point causes the loss of the

simplicity of the sparse matrices in the continuous-time domain. This generates a rise in computation time and complexity associated to the control. In order to reduce the complexity of the system and to decrease the computational effort, the system dimension is reduced to a more manageable 25 states. Although Equation (2) maintains its structure for the reduced system, the reduction implies the loss of the physical meaning of the states, so **y**, the output vector, is necessary to recover the information needed for the evaluation of the results.

The state-space model that defines the dynamics of the module is described for continuous representation as:

$$\begin{aligned} \dot{\boldsymbol{x}} &= \mathbf{A}\boldsymbol{x} + \mathbf{B}_u\boldsymbol{u} + \mathbf{B}_v\boldsymbol{v} + \mathbf{B}_{uv}\boldsymbol{u}_{\mathrm{BS}}\boldsymbol{v} \\ \boldsymbol{y} &= \mathbf{C}\boldsymbol{x} + \mathbf{D}_u\boldsymbol{u} + \mathbf{D}_v\boldsymbol{v} + \mathbf{D}_{uv}\boldsymbol{u}_{\mathrm{BS}}\boldsymbol{v} \end{aligned} \tag{2}$$

where $\boldsymbol{x} \in \mathbb{R}^{\mathrm{n}_x}$ is the state vector and n_x the number of states, $\boldsymbol{u} \in \mathbb{R}^{\mathrm{n}_u}$ is the control action of the HVAC system with n_u actuators (2 TABS and 3 AHU) and $\boldsymbol{v} \in \mathbb{R}^{\mathrm{n}_v}$ is the vector that represents the n_v disturbances in the system: outdoor temperature, solar radiation for north and south orientation, internal gains associated to human activity in the office. Vector $\boldsymbol{y} \in \mathbb{R}^{\mathrm{n}_y}$ contains the n_y values observed in the system. $\mathbf{A}$, $\mathbf{B}_u$, $\mathbf{B}_v$, $\mathbf{B}_{uv}$, $\mathbf{C}$, $\mathbf{D}_u$, $\mathbf{D}_v$, $\mathbf{D}_{uv}$ are the matrices that define the system. $\mathbf{A} \in \mathbb{R}^{\mathrm{n}_x \times \mathrm{n}_x}$ defines system dynamics, $\mathbf{B}_u \in \mathbb{R}^{\mathrm{n}_x \times \mathrm{n}_u}$ represents the effect of the control action on the system, $\mathbf{B}_v \in \mathbb{R}^{\mathrm{n}_x \times \mathrm{n}_v}$ determines the effect of the disturbances on the system and $\mathbf{B}_{uv} \in \mathbb{R}^{\mathrm{n}_x \times \mathrm{n}_{\mathrm{BS}}}$ determines the influence of the solar radiation among the windows where n_{BS} is the BS number. $\boldsymbol{u}_{\mathrm{BS}} \in \mathbb{R}^{\mathrm{n}_{\mathrm{BS}} \times \mathrm{n}_v}$ is the matrix associated with the action of the BSC. $\mathbf{C} \in \mathbb{R}^{\mathrm{n}_y \times \mathrm{n}_x}$, $\mathbf{D}_u \in \mathbb{R}^{\mathrm{n}_y \times \mathrm{n}_u}$, $\mathbf{D}_v \in \mathbb{R}^{\mathrm{n}_y \times \mathrm{n}_v}$ and $\mathbf{D}_{uv} \in \mathbb{R}^{\mathrm{n}_y \times \mathrm{n}_{\mathrm{BS}}}$ give the values of the system states making it observable. The action of the solar radiation is decoupled; the effect of the solar radiation over the façade is represented in $\mathbf{B}_v$ matrix, meanwhile the nonlinear term $\mathbf{B}_{uv}\boldsymbol{u}_{\mathrm{BS}}\boldsymbol{v}$ determines the influence of the BS and the solar radiation among the windows, in which vector $\boldsymbol{v}$ contains the solar radiation value and $\boldsymbol{u}_{\mathrm{BS}}$ is the BS control action that limits the solar radiation when closed. The discrete-reduced state-space model also maintains this representation.

3.1.2. State-Space Model Reduction

The reduction of the number of states of the state-space model is performed using a balanced model truncation via square root method. For an n order continuous or discrete state-space system:

$$\begin{aligned} \dot{\boldsymbol{x}} &= \mathbf{A}\boldsymbol{x} + \mathbf{B}\boldsymbol{u} \\ \boldsymbol{y} &= \mathbf{C}\boldsymbol{x} + \mathbf{D}\boldsymbol{u} \end{aligned} \tag{3}$$

where $\boldsymbol{x} \in \mathbb{R}^n$ and $\boldsymbol{u} \in \mathbb{R}^m$.

It is possible to obtain a reduced k order system:

$$\begin{bmatrix} \hat{\mathbf{A}} & \hat{\mathbf{B}} \\ \hat{\mathbf{C}} & \hat{\mathbf{D}} \end{bmatrix} = \begin{bmatrix} \mathbf{T}^{-1}\mathbf{A}\mathbf{T} & \mathbf{T}^{-1}\mathbf{B} \\ \mathbf{C}\mathbf{T} & \mathbf{D} \end{bmatrix} \tag{4}$$

where $\mathbf{T} \in \mathbb{R}^{n \times k}$ is the transformation matrix which performs an invertible state-space transformation, using the square root method as described by Safonov and Chiang in [48].

For the system, it is possible to obtain the singular value decomposition (SVD) of the controllability and observability grammians $\mathbf{P}$ and $\mathbf{Q}$:

$$\begin{aligned} \mathbf{P} &= \mathbf{U}_{\mathrm{p}}\boldsymbol{\Sigma}_{\mathrm{p}}\mathbf{V}_{\mathrm{p}}^{\mathrm{T}} \\ \mathbf{Q} &= \mathbf{U}_{\mathrm{q}}\boldsymbol{\Sigma}_{\mathrm{q}}\mathbf{V}_{\mathrm{q}}^{\mathrm{T}} \end{aligned} \tag{5}$$

$\mathbf{U}_{\mathrm{p}}$, $\mathbf{V}_{\mathrm{p}}$ and $\mathbf{U}_{\mathrm{q}}$, $\mathbf{V}_{\mathrm{q}}$ are mutually orthogonal.

Let the square root of the grammians (left/right eigenvectors) be:

$$\begin{aligned} \mathbf{L}_{\mathrm{o}} &= \mathbf{U}_{\mathrm{q}}\boldsymbol{\Sigma}_{\mathrm{q}}^{1/2} \\ \mathbf{L}_{\mathrm{p}} &= \mathbf{U}_{\mathrm{p}}\boldsymbol{\Sigma}_{\mathrm{p}}^{1/2} \end{aligned} \tag{6}$$

and the SVD of $\mathbf{L}_{\mathrm{o}}^{\mathrm{T}}\mathbf{L}_{\mathrm{p}}$, $\boldsymbol{\Sigma}$:

$$\mathbf{L}_{\mathrm{o}}^{\mathrm{T}}\mathbf{L}_{\mathrm{p}} = \mathbf{U}\boldsymbol{\Sigma}\mathbf{V}^{\mathrm{T}} \tag{7}$$

where $\boldsymbol{\Sigma} = \mathrm{diag}(\sigma_1, \ldots, \sigma_k) \in \mathbb{R}^{k\times k}$.

Then, the left and right transformation for the final kth order reduced model truncated for the largest singular values are:

$$\begin{aligned} \mathbf{S}_{\mathrm{L,BIG}} &= \mathbf{L}_{\mathrm{o}}\mathbf{U}\begin{bmatrix} \boldsymbol{\Sigma}^{-1/2} \\ \mathbf{0} \end{bmatrix} \in \mathbb{R}^{n\times k} \\ \mathbf{S}_{\mathrm{R,BIG}} &= \mathbf{L}_{\mathrm{p}}\mathbf{V}\begin{bmatrix} \boldsymbol{\Sigma}^{-1/2} \\ \mathbf{0} \end{bmatrix} \in \mathbb{R}^{n\times k} \end{aligned} \tag{8}$$

where $\mathbf{S}_{\mathrm{L,BIG}}$ and $\mathbf{S}_{\mathrm{R,BIG}}$ are the first k columns of $\mathbf{T}^{-\mathrm{T}}$ and $\mathbf{T}$ transformation matrices.

The reduced system becomes:

$$\begin{bmatrix} \hat{\mathbf{A}} & \hat{\mathbf{B}} \\ \hat{\mathbf{C}} & \hat{\mathbf{D}} \end{bmatrix} = \begin{bmatrix} \mathbf{S}_{\mathrm{L,BIG}}^{\mathrm{T}}\mathbf{A}\mathbf{S}_{\mathrm{R,BIG}} & \mathbf{S}_{\mathrm{L,BIG}}^{\mathrm{T}}\mathbf{B} \\ \mathbf{C}\mathbf{S}_{\mathrm{R,BIG}} & \mathbf{D} \end{bmatrix} \tag{9}$$

with an error bound on the infinity norm of the additive error for well-conditioned model reduction:

$$\| \mathbf{G} - \mathbf{G}_{\mathrm{red}} \|_{\infty} \leq 2\sum_{k+1}^{n}\sigma_i \tag{10}$$

where $\mathbf{G}$ and $\mathbf{G}_{\mathrm{red}}$ are the initial and reduced system and n and k their respective orders.

3.2. Control

3.2.1. Main Control of the Heating, Ventilating and Air-Conditioning System: Model Predictive Control (MPC)

To avoid an undesired frequent switching between hot and cold activation of the TABS, the control defines a seasonal TABS action. Based on the meteorological forecast of a characteristic Belgian year for outside temperature and solar irradiance, the TABS is designated for cooling from spring to the middle of autumn and for heating during the rest of the year. In addition to meeting the needs of ventilation and humidity, the AHU will satisfy the need for additional heating or cooling power necessary to maintain the thermal comfort.

The control algorithm set aims to maintain the indoor temperature of the office zones and corridor within the thermal comfort requirements. The control actuators are TABS and AHU on the one hand and the BS on the other hand. TABS and AHU condition office zones and corridor, while the BS controls the solar radiation. In order to increase the energy savings and reduce the complexity of the system, the main MPC does not integrate the BSC, although communication between both controls exists. The integration of the BS in the MPC would increase the global energy use, which may be observed from the results of Section 4.

The main climate control implements an MPC, a multi-objective advanced control that must maintain the comfort conditions while minimizing the energy use. The MPC controls the HVAC actions of the TABS and the AHU taking into account the perturbations at the evaluation moment as well as those in a future period denoted by the prediction horizon, Np. Figure 3 shows a scheme of an MPC applied to control the comfort conditions of a building.

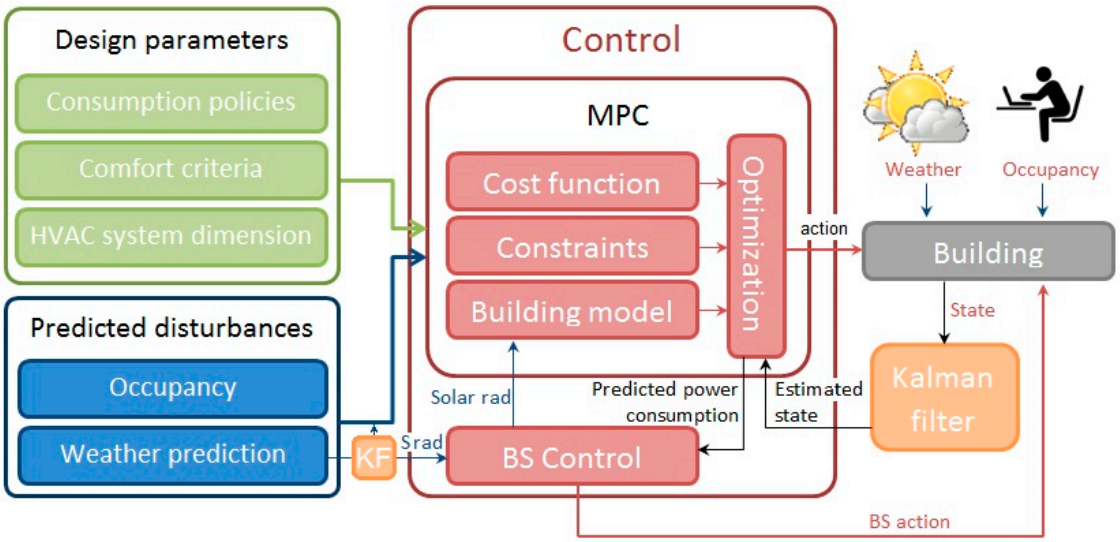

Figure 3. Model Predictive Control (MPC) scheme of the control for the the Heating, Ventilating and Air-Conditioning (HVAC) system of a building with the proposed enhanced Blind System Control (BSC).

As mentioned in the introduction, the use of an MPC can realise an improvement of 15% or more in energy savings compared to other controls such as Rule Based Control, RBC, that are widely used in HVAC control. Provided with the state-space model of the building, the MPC uses measured and predicted disturbances that influence the system to calculate the control action. The minimization of a cost function for the $\boldsymbol{u}$ vector is a typical constrained quadratic programming problem represented by Equation (11) with a prediction horizon Np subject to the constraints given by Equations (12)–(14). The solution of the minimization provides the minimum action the HVAC system needs to guarantee the thermal comfort in the building.

$$\min_{\boldsymbol{u}_0 \ldots \boldsymbol{u}_{\mathrm{Np}-1}} \sum_{\mathrm{k}=0}^{\mathrm{N_p}-1} \left(\left(\boldsymbol{\omega} - \boldsymbol{y}_{office} \right)_{\mathrm{k}}^{\mathrm{T}} \mathbf{Q} \left(\boldsymbol{\omega} - \boldsymbol{y}_{office} \right)_{\mathrm{k}} + \boldsymbol{u}_{\mathrm{k}}^{\mathrm{T}} \mathbf{R} \boldsymbol{u}_{\mathrm{k}} \right) \tag{11}$$

where $\boldsymbol{y}_{office} = (\mathrm{T_{north}}, \mathrm{T_{corridor}}, \mathrm{T_{south}})^{\mathrm{T}} \subset \boldsymbol{y}$ is the vector that stores the indoor temperatures of the office zones and corridor, which is a subset of vector $\boldsymbol{y}$, outputs of the system, $\boldsymbol{\omega}$ is the vector of temperature references for office zones and corridor. $\boldsymbol{u}$ is the vector that provides the control actions (energy use). $\mathbf{Q} \in \mathbb{R}^{\mathrm{n}_{y\_office} \times \mathrm{n}_{y\_office}}$, with n_{y_office} the number of controlled temperatures, and $\mathbf{R} \in \mathbb{R}^{\mathrm{n}_u \times \mathrm{n}_u}$ are diagonal positive semidefinite matrices that weigh the deviation from the reference temperature and the energy use in the minimization, and k is the evaluated time moment of the prediction horizon.

The system is subject to the following constraints:

$$\mathbf{MinPower}_{\mathrm{k}} < \boldsymbol{u}_{\mathrm{k}} < \mathbf{MaxPower}_{\mathrm{k}} \tag{12}$$

$$\mathbf{T}_{\mathrm{min,k}} < \boldsymbol{y}_{\mathrm{in,k}} < \mathbf{T}_{\mathrm{max,k}} \tag{13}$$

$$\mathbf{T}_{\mathrm{surfmin,k}} < \boldsymbol{y}_{\mathrm{surf,k}} < \mathbf{T}_{\mathrm{surfmax,k}} \tag{14}$$

where **MinPower** and **MaxPower** determine the minimum and maximum power values the HVAC system can supply. $\boldsymbol{y}_{\mathrm{in}}$ denotes the temperature in the office zones and corridor limited by the boundary values of the comfort band $\mathbf{T}_{\mathrm{min}}$ and $\mathbf{T}_{\mathrm{max}}$. $\boldsymbol{y}_{\mathrm{surf}}$ is the temperature of the surface of the ceiling and floor where $\mathbf{T}_{\mathrm{surfmin}}$ and $\mathbf{T}_{\mathrm{surfmax}}$ delimit its range of values to avoid overheating and condensation of moisture at inner surfaces.

The MPC calculates the optimal action over the prediction horizon using the weights associated to the variables, the reference for the indoor temperature and the defined constrains. The minimization problem is the core of the MPC and provides a control vector for the time horizon that will fulfil the desired conditions under the predicted disturbances. For each iteration, the control action only implements the first element discarding the rest, recalculating the next series of control actions in the next iteration. In the case investigated, CPLEX [49] is used as solver with YALMIP [50] to construct the problem. YALMIP provides high freedom in the design of the minimization problem as well as an improved efficiency in computational resources. As a design choice, the control prioritizes the use of the TABS above the AHU using the weights inside the **R** diagonal matrix, Equation (11). These weights ideally reflect the real operating cost associated to both systems. The relationship between the weights associated to the energy use, **R**, and those related to the deviation of the indoor temperature from the reference temperatures, **Q**, defines different energy use policies, allowing a deviation from the reference temperature when it can provide important energy savings.

The MPC is not only defined by the cost function and the weights associated to the different terms that appear in the cost function. A definition of the physical power limits of the HVAC and of the comfort bounds is also necessary, as shown in Equations (12)–(14). Moreover, the weather conditions may force the system outside of the comfort bounds, which can provoke problems when looking for an optimum within the given constrains. In order to avoid this situation, which does not lead to a solution, and to add robustness to the control, the bounds of the comfort band defined in Equation (13) are relaxed as:

$$\mathbf{T}_{\mathrm{min,k}} - \boldsymbol{\varepsilon}_{\mathrm{k}} < \boldsymbol{y}_{\mathrm{in,k}} < \mathbf{T}_{\mathrm{max,k}} + \boldsymbol{\varepsilon}_{\mathrm{k}} \tag{15}$$

$$\boldsymbol{\varepsilon}_{\mathrm{k}} > 0 \tag{16}$$

where $\boldsymbol{\varepsilon}_{\mathrm{k}}$ is a highly weighted relaxation variable of the minimization that allows the temperature to trespass the comfort limits. Thus, the minimization may be rewritten as:

$$\min_{\boldsymbol{u}_0 \ldots \boldsymbol{u}_{\mathrm{N_p}-1}} \sum_{\mathrm{k}=0}^{\mathrm{N_p}-1} \left((\boldsymbol{\omega} - \boldsymbol{y})_{\mathrm{k}}^{\mathrm{T}} \mathbf{Q} (\boldsymbol{\omega} - \boldsymbol{y})_{\mathrm{k}} + \boldsymbol{u}_{\mathrm{k}}^{\mathrm{T}} \mathbf{R} \boldsymbol{u}_{\mathrm{k}} + \boldsymbol{\varepsilon}_{\mathrm{k}}^{\mathrm{T}} \mathbf{S} \boldsymbol{\varepsilon}_{\mathrm{k}} \right) \tag{17}$$

where $\mathbf{S} \in \mathbb{R}^{\mathbf{n}_\varepsilon \times \mathbf{n}_\varepsilon}$ is the weight matrix associated to the $\boldsymbol{\varepsilon}$ parameter, its values being significantly larger than the ones of **Q** and **R**.

As the system prioritizes the use of the TABS over the AHU, the system is subject to one last constraint: the use of the AHU is restricted to office hours.

3.2.2. Blind System

The characteristics of the MPC that provide the control actions for the TABS and AHU so that the office zones remain inside the thermal comfort conditions have been described in the previous subsection. The difference between the time constants of BS and climate system hinders the implementation of the BSC as another control action of the MPC. For this reason, the control action of the BS is kept separate from the MPC and is implemented as a distributed control. This subsection introduces the complete control of the climate system as an MPC enhanced with a BS control.

The main objective of this study is the design of a distributed, simple and effective control for the BS, compatible with the predictive capacities of the main MPC. The blinds must stay open if the incident solar irradiance is lower than 150 W/m^2 [33], which allows all the incident radiation to pass through. The blinds must be closed if the solar irradiance is higher than 250 W/m^2, which reduces the passing radiation through BS to 25% of the incident one, as explained in Table 4. Therefore, the value of the solar radiation that the MPC computes over a window, S_rad_{MPC}, is defined by:

$$S\_rad_{MPC} = u \cdot S\_rad \tag{18}$$

where $u \in \{0.25,\ 1\}$ defines the BSC action.

Table 4. BS state related to the incident solar radiation (*S_rad*) and solar radiation value through BS.

Solar Radiation	BS State	Solar Radiation after BS
Solar radiation > 250 W/m^2	CLOSED	0.25· *S_rad*
150 W/m^2 < Solar radiation < 250 W/m^2	BSC defined	***u***·*S_rad*
Solar radiation < 150 W/m^2	OPEN	*S_rad*

The lack of definition of the BS state for the intermediate irradiance values allows different control strategies that condition the energetic behaviour of the building. In order to keep the BS hardware and control as simple as possible, the allowed states for the system are either open or closed with no intermediate positions.

Previous studies that focused on the behaviour of the climate system have implemented the BS as an On-Off hysteresis control, hysteresis BSC. The results obtained using that control will be compared with the ones from a novel enhanced BSC, in order to illustrate the benefits of that novel BSC. The enhanced BSC will use the predicted results of the main MPC. As the prediction horizon period is too long for the BSC, two-hour ahead-predicted results will be used only, which is substantially shorter than the prediction horizon of the MPC, but long enough to be significant. Predicted energy use is the main indicator to determine the BS control action. If there is net heat use for the next two hours, the BSC will open the blinds, closing them when the prediction is cold use. The design of the enhanced BSC considers also the following assumptions:

- The BS stays closed if the incident irradiance is higher than 250 W/m^2. It will be open when the incident radiation is lower than 150 W/m^2.
- The BS action does not influence the illumination comfort of the office and there are no extra energy expenses when the blind system is closed. This simplification is also made by the hysteresis control.
- The design of the main MPC is identical for both enhanced and hysteresis BSC. The difference between them will be the amount of radiation that passes through each BS.
- In order to increase the user global comfort minimizing the action of the BS, when the predicted average power use in the TABS/AHU system for the next two hours is below a predefined threshold, the BS state remains unchanged.

3.2.3. Proposed Enhanced Blind System Control (BSC)

The design of an improved BSC system for the two office zones module enhances the global control behaviour of the climate system, both economically and energetically as well as from a comfort perspective.

Figure 4 shows the interaction of the novel enhanced BSC with the main MPC. The MPC evaluates the system for a control action during the prediction horizon using the values of the solar radiation among others. The BSC receives the information of the predicted solar radiation for the prediction horizon and the values of the control action of the previous iteration to decide about the need of heating or cooling of the office.

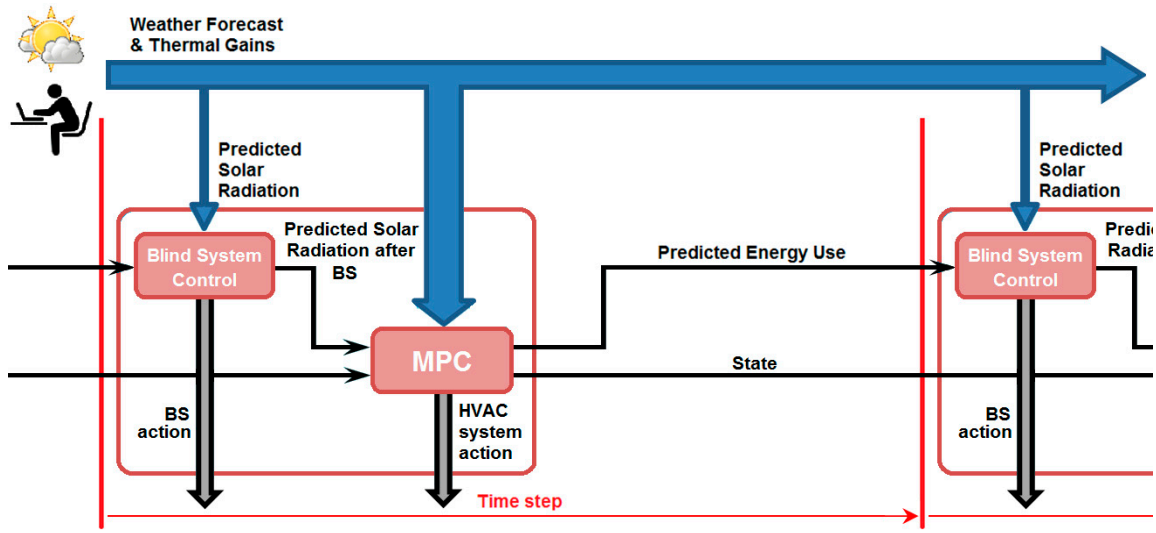

Figure 4. Scheme showing one of the interactions of the enhanced BSC with the main MPC control.

The BSC evaluates the solar irradiance at each time step of the prediction horizon. If the solar radiation is between 150 and 250 W/m^2 (the BS state is not predefined), the controller must determine the BS state for that step and give the MPC the recalculated solar irradiance value through the BS.

The control computes the predicted energy needs for the next two hours; the BS will be open in case of a net heating power demand, and closed if there is a demand for cooling power in order to assist the action of the main HVAC system. However, a small hysteresis band is imposed on the energy-use variable, during which the BS state is not changed to avoid consecutive opening and closing of the blinds that can disturb the office users' comfort. The MPC receives the information of the predicted solar radiation through the BS for the prediction horizon and using these values, calculates the control action for the HVAC to ensure comfort conditions and minimize energy use. Figure 5 shows a flow chart representing the behaviour of the BSC.

In order to study the efficiency of the enhanced BSC and the influence of the solar radiation, the control performance is compared with other BSCs under the same operating conditions. An MPC operates the HVAC system under the same parameters for all the simulations, except for the BS. Table 5 presents the temperature ranges that determine the comfort bands for heating in winter configuration, and cooling in summer.

Table 5. Reference values and comfort band limits for temperature (in °C). Office hours are considered from 08:00 to 18:00.

Comfort Definitions	Heating		Cooling	
	Office Hours	Night/Weekend	Office Hours	Night/Weekend
Upper temperature	22	22	26	26
Reference	20	no ref	24	no ref
Lower temperature	18	16	20	20

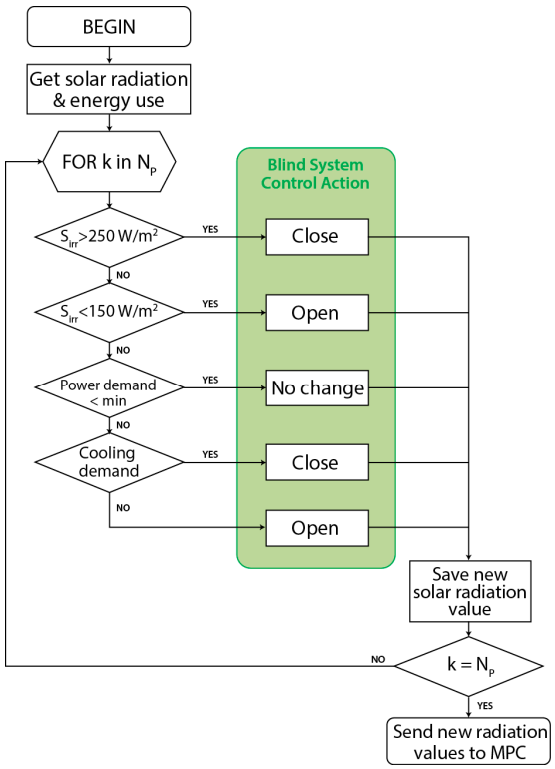

Figure 5. Flow chart representation of the proposed enhanced BSC.

When the TABS is configured for heating, the reference temperature during the day is 20 °C, with a comfort band of 2 °C below and above the reference. In order to reduce the energy use, there is no temperature reference during night and weekend time and the lower limit of the comfort band drops to 16 °C in these periods. Due to its predictive nature, MPC has no problem to recover the comfort band around the temperature reference at the beginning of the working day. Assuming adapted clothing during the cooling season; in summer, the values for the reference temperature during the day is raised to 24 °C and the upper and lower bounds of the comfort band are raised to 26 °C and 20 °C respectively. The MPC design provides the office zones both reference and comfort band while the design for the corridor, due to the thermal isolation from the exterior provided by the office zones, delimits the comfort band only. During no occupancy time, no reference is assumed in order to improve the energetic efficiency and the lower bound constriction is softened. Although the reference temperature can also be removed during occupation time, which would minimize the energy use making matrix **Q** in Equation (17) zero, the reference gives the control a more stable evolution inside the comfort band reducing discomfort from unforeseen disturbance changes. Modifying the weights in Equation (17) it is possible to prioritize energy savings giving the reference temperature a role to help stabilizing temperatures within the comfort band. The internal gains associated with the office use have a great influence on the system dynamics and have been defined earlier in Table 3.

3.3. Performance Indicators

3.3.1. Energy Use

Using an MPC as main HVAC control, the study focuses on the influence of the solar radiation on the comfort conditions and energy use. In this way, BS plays an important role because even when solar radiation helps to warm the office zones during winter, it negatively affects thermal comfort during summer and increases cost. Four scenarios are proposed to study and manage the effect of the solar radiation through the windows:

(1) No BS: This scenario is used as a reference. There is no BS to mitigate the influence of the solar radiation, so the MPC has to manage the HVAC to dissipate the energy of the solar radiation. This scenario should provide the worst situation with respect to energy use in summer. In winter, this would provide more heat gains improving the results, as long as this does not imply the need for cooling.

(2) Hysteresis BSC: This is a usually proposed control as shown in the already presented literature. The control action is defined by a hysteresis control when the solar radiation value is inside the limits defined in Table 4. The control action is open or close. It is presumed that the performance of this control can be improved.

(3) MPC integrated BSC: In this case, the MPC internalizes the BS. The minimization function, considers the action of the solar radiation as another minimization parameter when it is between the already defined maximum and minimum radiation values. The predictive capacity of the MPC ensures an appropriate control and, in order to improve the control response; the BS is not limited to open or closed positions, being able to stay in any other intermediate position. Considering the nature of the MPC, which minimizes the objective function for the whole prediction horizon, the effect of the absence of solar radiation at night can distort the results for the hours near the sunset, which could affect the total energy use.

(4) Enhanced MPC: This is the improved control proposed in this paper. It takes information about the predicted energy use for the future two hours and uses this information to define an open or close state for the controllable radiation band. This control is supposed to give upgraded results improving the behaviour of the hysteresis one.

The orientation of the offices introduces an important distinction between the solar radiation values: as will be seen, while the BS is nearly unnecessary in the north office during the whole year, its use in the south one is mandatory to reduce the amount of solar radiation that gets into the south office zone in summer.

Besides assuming that the control prioritizes the use of TABS for economic reasons, the increase of the use-ratio between TABS and AHU will supposedly imply an improvement in the system performance due to the possible usage of more efficient climate equipment as heat pumps.

In addition to the energy savings, some studies start to consider the expenses associated to the control hardware as well as other cost factors [32]. In the proposed novel strategy, there are no special hardware requirements aside from the already supposed On-Off automatization for the BS and the implementation of the proposed software is not expected to cause a significant increase of the computational effort compared to the MPC.

3.3.2. Thermal Comfort

Evaluation of the thermal comfort is also necessary. The comfort is supposed to be guaranteed inside the bands defined in Table 5. Outside these values, there is a thermal discomfort situation.

Although the use of the Predicted Mean Vote/Predicted Percentage of Dissatisfied (PMV/PPD) as defined in ASHRAE 55 is a common thermal discomfort standard and successful integration of the PMV index in MPC is described by Freire et al. [51], its nonlinear character still causes some difficulties in its use. In order to simplify the study, the unit selected to determine the thermal discomfort is the Kelvin hour (*Kh*), which is defined as the integration over time of the temperature surplus outside the comfort band. By adapting the comfort band values to the season it is possible to improve the feasibility of this method. The low deviation of the temperature from the comfort band has never been larger than 1 K for occupation period as will be seen in Section 4, which makes this unit a good option to evaluate the thermal comfort.

The evaluation of the discomfort value in a discrete system is based on the sum of the temperature deviation value out of the comfort band for all the time steps multiplied by the system discretization Ts in hours. This value is computed when the deviation is larger than 0.1 K. This is:

$$Kh = \sum_i \left|\Delta T_{dev,i} Ts_i\right| \qquad i \in \{occupation\ period\} \tag{19}$$

where ΔT_{dev} is the temperature deviation from the defined comfort band.

4. Results

4.1. Enhanced BSC Results

This Section shows the results obtained in the module of office zones under the different control schemes. The control must maintain the office module inside the thermal comfort conditions while using the minimum amount of energy. The study focuses on the savings that the use of a suitable BSC adds to the general MPC.

Figure 6 provides a year-long representation of the behaviour of the climate system in the two office zones and corridor using the enhanced control for the BS (scenario 4). The simulation results show the global behaviour of the system during the whole year; no BSC, hysteresis BSC and MPC integrated BSC lead to results similar to those in Figure 6, although an increase in energy use and thermal discomfort appears. It is possible to see how the control maintains the indoor temperature inside the defined comfort band. The inertia of the TABS and the thermal gains of the offices, human use and office devices, cause variations with respect to the reference temperature. In some occasions, the temperature exceeds the lower comfort limit due to the relaxation in the design of the comfort constraint when offices are out of use.

The energy use for both TABS and AHU also appears in Figure 6. Recall that the use of TABS is limited to heating in winter and to cooling in summer as the figure shows; while the AHU is designed to provide support action for heating or cooling as can be observed in Figure 6b column. It may therefore be observed from the accumulated energy use that the cold consumption exceeds the heat consumption, such that an adequate use of the BS will provide significant energy savings. The south office has higher solar exposure than the north one, which increases the cooling energy use. The temperature in the corridor remains quite stable, because of the regulating effect provided by the adjacent offices and the absence of significant heat gains. Therefore, it has been found that the BSC action is mainly focused on the south office.

Figure 7 zooms into the control response of Figure 6. A representative zoom of a week is shown for the TABS heating and cooling configuration for the south office. This shows the evolution of the temperature and the energy use of TABS and AHU. Control is fitted in order to improve the energy savings so the value of the weight matrix **Q**, associated to the energy use, has larger eigenvalues than the values of matrix **R**, associated to the reference tracking, in Equation (17), which entails that the control will not strictly follow the temperature reference. It is also possible to observe the effect of the ε parameter: the MPC allows the temperature to exceed the comfort band in some occasions in order to decrease the energy use. This is merely a design choice. The behaviour of the TABS and the delay associated to the heat transfer through the concrete can be observed. The thermal energy is mostly stored in the TABS at night to be used during the office hours. This delay also shows the predictive behaviour of the MPC. While TABS are in heating configuration, the AHU system is mainly used to correct the temperature deviations in cooling configuration as it provides additional cooling power when required. A temperature decrease appears at lunchtime. The lack of internal gains associated to occupancy and office appliances combined with the ventilation heat losses cause this to happen in both cooling and heating configurations. The lower graphs show the behaviour of the control under a *no discomfort* policy as compared to the power saving policy. Weights associated to the reference track and ε parameter in Equation (17) have been increased, putting a higher penalty on discomfort.

Using the parameters of the study, it is possible to maintain the temperature inside the comfort limits at the expense of increased energy use.

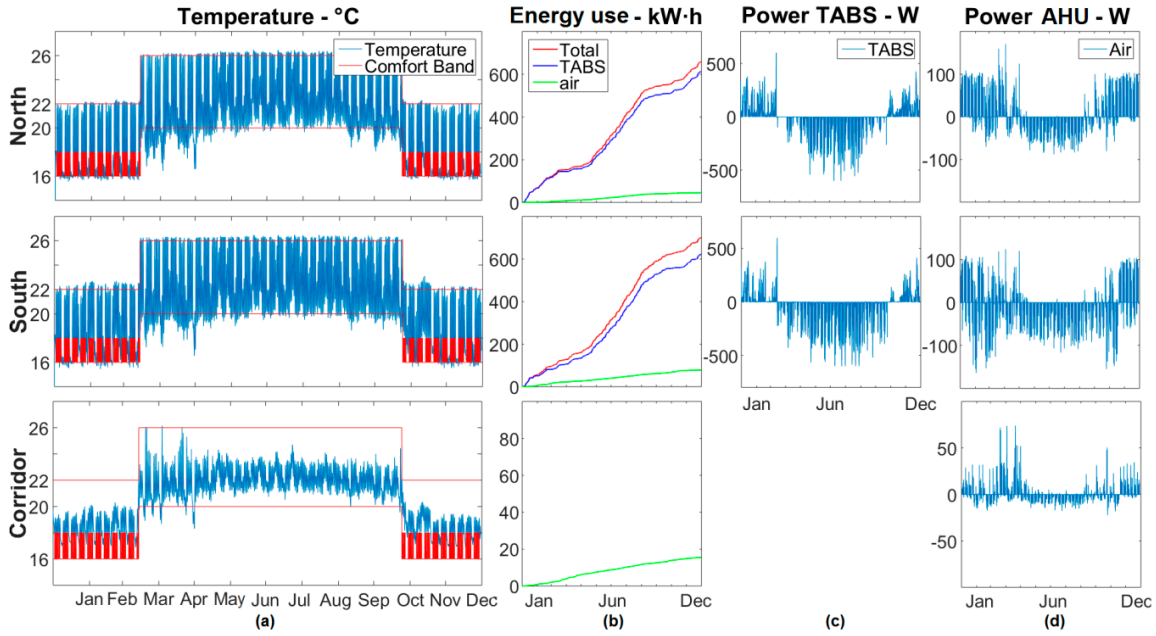

Figure 6. Enhanced BSC study: zone temperature evolution (**a**), accumulated energy use (**b**) and developed power in TABS (**c**) and in AHU (**d**).

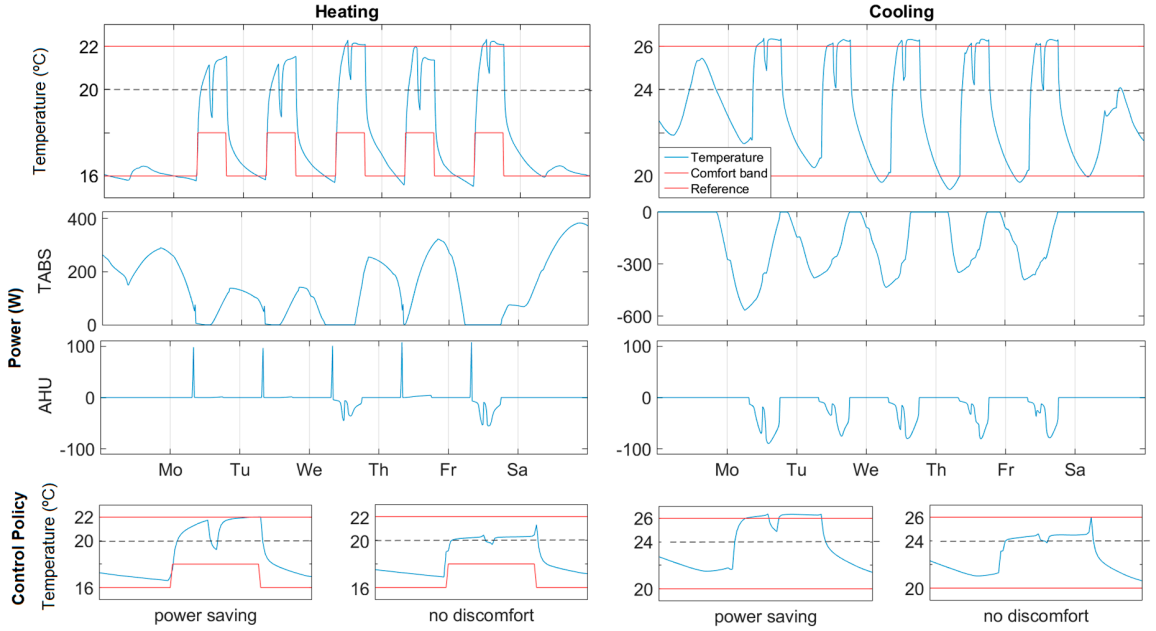

Figure 7. One-week response of the control for heating and cooling configurations. Temperature evolution, and TABS and AHU system power use are shown. One-day temperature evolution for the selected configuration, power saving, against a *no discomfort* policy is also presented at the bottom.

Figure 8 shows other aspects of the behaviour of the enhanced BSC. The action of the BS control can be observed in Figure 8a, which represents its state evolution over time. The other columns show the accumulated thermal discomfort in Kh.

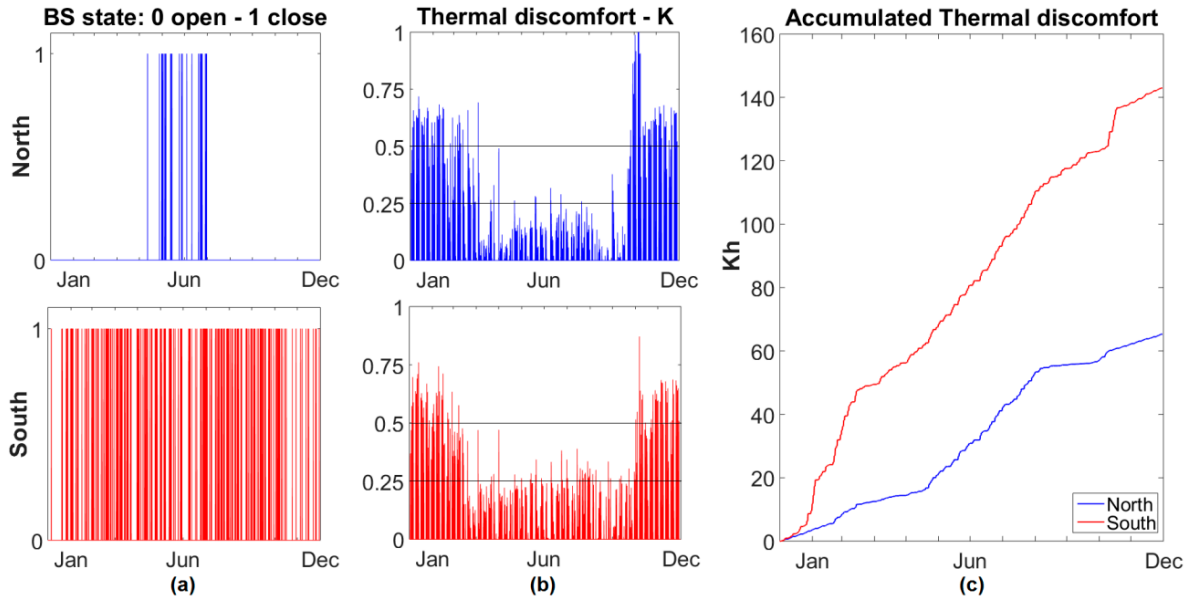

Figure 8. Enhanced BSC study. BS state (**a**), thermal discomfort (**b**) and accumulated thermal discomfort (**c**) for north and south offices.

The thermal discomfort in Kh is defined as the integration over time of the temperature surpassing outside the comfort band during occupation hours. In [18], Gyalistras et al. suggested values near 70 Kelvin hours per annum (Kh/a) as a good indicator for thermal discomfort. Only deviations larger than 0.1 K are considered when evaluating the discomfort, as suggested in [18]. Taking into account the distribution of the thermal discomfort over the year, Figure 8b, it can be seen that in the south office the temperature is only out of the comfort band during 0.65% of the office-time for a deviation higher than 0.5 K and it never surpasses 1 K. As result of these considerations, the outcomes for the control action are considered satisfactory, especially knowing that the MPC design allows to exceed of the comfort band as denoted by Equation (17).

Figure 9 presents a comparison between the enhanced BSC and the other three BSC scenarios defined in Section 3.3.1: hysteresis BSC, the MPC integrated control and no BS control. The response patterns of Figures 6 and 7 are similar for all these controls, so the comparison is based on the accumulated energy use as well as the accumulated thermal discomfort in Kh for the four cases over a whole year.

The graphics in Figure 9a show that the enhanced BSC provides the lowest energy use and the highest comfort (Figure 9b) for the south oriented office zone, whereas the north office zone presents similar results for all four BSCs (Figure 9c,d). Besides, according to Figure 9a, major savings are accumulated during the cooling period, when the solar radiation maximizes its influence. In particular, the novel enhanced BSC presents an overall energy use, which is 15% lower than the hysteresis BSC, and similar energy use results to the MPC integrated BSC. Regarding thermal discomfort, it can be observed in Figure 9d that there is no substantial difference between BSC actions in north orientation. For South orientation, the enhanced BSC and MPC integrated BSC show similar results, which are better than the hysteresis one in Figure 9b.

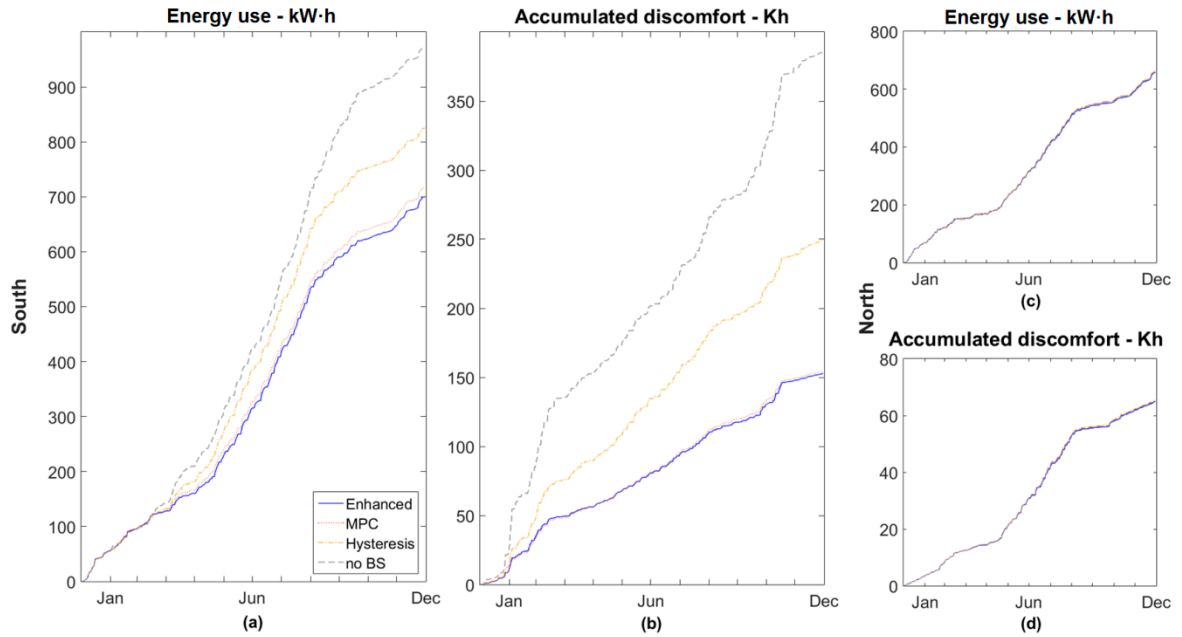

Figure 9. Accumulated energy use (**a**,**c**) and thermal discomfort (**b**,**d**) in north and south office orientations for the studied controls.

4.2. Enhanced BSC Results. Interpretation and Discussion

The simulation results indicate that most of the energy savings associated to the use of the enhanced BSC occur in the south office during the summer period. The large influence that internal gains exert on the environment induces a heavy use of the cooling system. The effect of solar radiation, which can be observed comparing the results between north and south offices, increases the use of the cooling system. Therefore, a more active well-fitted BSC yields important savings in the energy use as Table 6 shows.

Table 6. Accumulated energy use of the HVAC system when different BSC are used. Energy use is referenced to the scenario without BS.

Scenario		Accumulated Energy Use kW·h					
		Total	**Winter**	**Summer**	**Energy Use (%)**	**Total TABS**	**Total AHU**
North	enhanced	659.0	257.8	401.0	99.54	613.2	45.8
	MPC	660.5	258.2	402.3	99.79	614.7	45.8
	hysteresis	664.1	256.5	407.5	100.32	618.0	46.1
	No_BS	662.0	253.0	408.9	100	615.8	46.2
South	enhanced	699.8	197.3	502.4	71.97	621.2	78.6
	MPC	716.8	198.5	518.2	73.73	637.4	79.4
	hysteresis	824.8	190.8	633.9	84.83	715.7	109.2
	No_BS	972.3	198.6	773.6	100	820.9	151.4

Due to the low solar radiation that the north office receives, the BSC has no relevance in the energy use. However, in the south oriented office the heating effect of solar radiation causes a substantial decrease in the energy use of 20% during the winter period, compared to the north office. Analysing the summer period, this passive heating effect increases the energy use for cooling. The maximum energy use occurs when no BS is present. The use of a hysteresis BSC reduces this energy use to 85% of the reference case. The integration of the BSC in the MPC or the use of the enhanced BSC reduces the energy use down to 74% and 72% of the reference case, respectively. Considering a whole year, the use of the enhanced BSC in the south office reduces the energy use to values close to those of

the north office, so that the control avoids the undesired heating effect of solar radiation in summer. This provides energy savings of 30% with respect to a no BS situation or 15% with respect to the hysteresis BS. When comparing with the MPC integrated control, there is only a small difference, but it must be considered that MPC requires a more complex hardware implementation than the enhance BSC.

The priority in the use of TABS over the AHU is defined in the MPC assuming different operative costs per unit of cooling or heating power. Using the enhanced BSC, the energy-use of TABS to AHU ratio is near 8, while this ratio decreases to 6.5 for the hysteresis control and 5.5 when no BS is present.

Results presented in Figure 8 and Table 7 give an idea about the thermal comfort provided to the users of the offices. Under the same study conditions, except for the parameters directly related to the BS, all other parameters of the MPC remain the same for all simulations. The enhanced BSC obtains the highest comfort. As in the previous comparison, MPC integrated BSC results are close to the ones of the enhanced BSC, while the usually proposed hysteresis shows worse behaviour. Results for the case without BS are the worst due to the increment of the energy use needed to maintain thermal comfort.

Table 7. Accumulated thermal discomfort in the south oriented office zone for the whole year and fraction of office time out of the comfort band for different temperature deviations.

Scenario	Thermal Discomfort Kh/a	Deviation > 0.25 K (%)	Deviation > 0.5 K (%)	Deviation > 1 K (%)
Enhanced	142.92	6.34	0.65	0
MPC integrated	154.04	6.48	0.71	0
Hysteresis	249.01	15.11	2.66	0
No_BS	385.12	21.28	9.19	1.39

In the south office, the BS mitigates the influence of solar radiation on thermal discomfort reducing discomfort when enhanced BS or MPC integrated BS is used. Figure 7 shows how to implement a *no discomfort* policy in which the temperature reference track and ε value weight are prioritized over energy use. The comfort is increased however also the energy use increases as can be deduced from Equation (17).

The use of the enhanced BSC provides significantly better results than those obtained with the usually proposed hysteresis BSC when evaluating both energy use and thermal comfort. Compared to the BS integration in the MPC, it shows similar results in thermal comfort and energy use, but the enhanced BSC simplifies the computational effort and the hardware complexity associated to the BS positioning. For a whole year calculation, an i7-6700 16 GB RAM desktop computer takes 8 h (24 h in the case of an i7-3520M 4 GB RAM laptop) for enhanced and hysteresis control calculation increasing this with about half an hour for the integrated MPC. The use of discrete BS positions in an integrated MPC, as the ones proposed in the literature, requires the use of integer programming that can increase the computation time more than an order of magnitude.

5. Conclusions

The climatization of office buildings represents an important fraction of the total energy use in our society. Besides conditioning the indoor air quality, the system must provide thermal comfort to the users. The use of an MPC gives rise to energy savings of about 15% with respect to traditional control policies.

The power dissipation of electronic devices in present-day offices provides heat gains, which together with human activity and solar radiation introduces heat sources that will significantly increase the temperature in the office zones. Although all these energy sources, considered in the HVAC control, reduce the heat power consumption during winter, they substantially increase the cooling needs in summer. This study investigates an office module, designed with high quality building materials and a solar BS, allowing decreasing the total use of energy of an MPC controlled HVAC system by simulations. The simulations for a novel enhanced BS algorithm decoupled from the MPC, but considering its predicted energy use values, provide a potential energy use reduction for the

HVAC system of 15% in comparison with a usually proposed hysteresis control. The evaluation of the predicted energy need provides a good indicator to determine the state of the BS.

The proposed control shows similar results for energy use and thermal comfort to an MPC that integrates the BS under similar conditions, which in some of its variants has been successfully studied. Therefore, the obtained results can be considered significant. The use of a decoupled control reduces computational requirements in the MPC minimization; meanwhile On-Off BS hardware is potentially simpler than multistate one.

Unlike the outside temperature or the heat gains associated with occupancy, the strong effect of solar radiation on thermal comfort, mostly in summer, can be counteracted. The development of an appropriate BSC provides an opportunity to significantly decrease the energy use, which justifies this study and the use of an advanced control strategy. The enhanced BSC also improves the distribution of the energy use over the two HVAC systems, TABS and AHU, which should entail a cost reduction by favouring the system with lower running costs.

The comparison among the different BSCs has been carried out considering perfectly known predictions for the disturbances. Deviations between the predicted and real values of solar radiation can introduce errors in the behaviour of the BSC. Therefore, once the control feasibility has been validated when comparing with other BSCs, future studies should contemplate the implementation under real conditions, taking into account on-line weather forecast predictions. In this case, a state estimation Kalman filter should be used to reduce the errors in the predictions. The study of the proposed BSC in other weather conditions or other qualities of the construction materials can also continue this research work.

Acknowledgments: This work was supported in part by the University of the Basque Country (UPV/EHU) through Project GIU14/07 and by the Basque Government through Project IT987-16, as well as by the MINECO through the Research Project DPI2015-70075-R (MINECO/FEDER). The work of Bram van der Heijde is funded by the European Union, the European Regional Development Fund ERDF, Flanders Innovation & Entrepreneurship and the Province of Limburg (Belgium) through the project EFRO Project 936 "Towards a Sustainable Energy Supply in Cities". The authors also want to recognize Maarten Sourbron, Damien Picard and Stefan Antonov from The SySis of KU Leuven for their support in the investigation.

Author Contributions: All authors have been involved in the preparation of the manuscript. Edorta Carrascal-Lekunberri prepared the manuscript and carried out the studies in this paper. Izaskun Garrido collaborated in the design and elaboration of the manuscript as well as in its supervision. Bram van der Heijde contributed to revision of the manuscript and to preparation of some of the illustrations. Aitor J. Garrido contributed to revision of the manuscript and provided some ideas about the control. José María Sala contributed to revision of the manuscript. Lieve Helsen provided the idea for the manuscript and supervised the initial work. She also contributed to design and revision of the manuscript.

Conflicts of Interest: The authors declare no conflict of interest.

Abbreviations

The following abbreviations are used in this manuscript:

ACH	Air Changes per Hour
AHU	Air Handling Unit
ANN	Artificial Neural Network
ASHRAE	American Society of Heating, Refrigerating and Air-Conditioning Engineers
BS	Blind System
BSC	Blind System Control
CCA	Concrete Core Activation
HVAC	Heating, Ventilating and Air-Conditioning
Kh	Kelvin hour
Kh/a	Kelvin hour per annum
MPC	Model Predictive Control

PI	Proportional Integral
PMV	Predicted Mean Vote
PPD	Predicted Percentage of Dissatisfied
TABS	Thermally Activated Building System
Ts	Time step

References

1. Bisegna, F.; Mattoni, B.; Asdrubali, F.; Guattari, C.; Evangelisti, L.; Sambuco, S.; Bianchi, F. Influence of insulating materials on green building rating system results. *Energies* **2016**, *9*, 712. [CrossRef]
2. Koschenz, M.; Lehmann, B. *Thermoaktive Bauteilsysteme TABS*; EMPA: Dübendorf, Switzerland, 2000.
3. Weber, T.; Jóhannesson, G.; Koschenz, M.; Lehmann, B.; Baumgartner, T. Validation of a FEM-program (frequency-domain) and a simplified RC-model (time-domain) for thermally activated building component systems (TABS) using measurement data. *Energy Build.* **2005**, *37*, 707–724. [CrossRef]
4. Weber, T.; Jóhannesson, G. An optimized RC-network for thermally activated building components. *Build. Environ.* **2005**, *40*, 1–14. [CrossRef]
5. Sourbron, M.; De Herdt, R.; Van Reet, T.; Van Passel, W.; Baelmans, M.; Helsen, L. Efficiently produced heat and cold is squandered by inappropriate control strategies: A case study. *Energy Build.* **2009**, *41*, 1091–1098. [CrossRef]
6. Gwerder, M.; Lehmann, B.; Tödtli, J.; Dorer, V.; Renggli, F. Control of thermally-activated building systems (TABS). *Appl. Energy* **2008**, *85*, 565–581. [CrossRef]
7. Yu, M.G.; Nam, Y. Study on the optimum design method of heat source systems with heat storage using a genetic algorithm. *Energies* **2016**, *9*, 849. [CrossRef]
8. Canbay, C.S.; Hepbasli, A.; Gokcen, G. Evaluating performance indices of a shopping centre and implementing HVAC control principles to minimize energy usage. *Energy Build.* **2004**, *36*, 587–598. [CrossRef]
9. Hamdi, M.; Lachiver, G. A fuzzy control system based on the human sensation of thermal comfort. In Proceedings of the IEEE International Conference on Fuzzy Systems, Anchorage, AK, USA, 4–9 May 1998; Volume 1, pp. 487–492.
10. Moon, J.W.; Lee, J.; Kim, S. Evaluation of artificial neural network-based temperature control for optimum operation of building envelopes. *Energies* **2014**, *7*, 7245–7265. [CrossRef]
11. Killian, M.; Mayer, B.; Kozek, M. Cooperative fuzzy model predictive control for heating and cooling of buildings. *Energy Build.* **2016**, *112*, 130–140. [CrossRef]
12. Richalet, J.; Rault, A.; Testud, J.L.; Papon, J. Model predictive heuristic control: Applications to industrial processes. *Automatica* **1978**, *14*, 413–428. [CrossRef]
13. Garrido, I.; Garrido, A.; Romero, J.; Carrascal, E.; Sevillano-Berasategui, G.; Barambones, O. Low effort L_i nuclear fusion plasma control using model predictive control laws. *Math. Probl. Eng.* **2015**, *2015*, 527420. [CrossRef]
14. Garrido, I.; Garrido, A.J.; Coda, S.; Le, H.B.; Moret, J.M. Real time hybrid model predictive control for the current profile of the Tokamak à configuration variable (TCV). *Energies* **2016**, *9*, 609. [CrossRef]
15. Singh, L.; Fuller, J. Trajectory Generation for a UAV in Urban Terrain, using Nonlinear MPC. In Proceedings of the American Control Conference, Arlington, VA, USA, 25–27 June 2001.
16. Ji, Z.; Huang, X.; Xu, C.; Sun, H. Accelerated model predictive control for electric vehicle integrated microgrid energy management: A hybrid robust and stochastic approach. *Energies* **2016**, *9*, 973. [CrossRef]
17. Hovorka, R.; Canonico, V.; Chassin, L.J.; Haueter, U.; Massi-Benedetti, M.; Orsini Federici, M.; Pieber, T.R.; Schaller, H.C.; Schaupp, L.; Vering, T.; et al. Nonlinear model predictive control of glucose concentration in subjects with type 1 diabetes. *Physiol. Meas.* **2004**, *25*, 905–920. [CrossRef] [PubMed]
18. Gyalistras, D.; Gwerder, M. Use of Weather and Occupancy Forecasts for Optimal Building Climate Control (OptiControl): Two Years Progress Report. Siemens Switzerland Ltd.: Zug, Switzerland, 2009. Available online: http://www.opticontrol.ethz.ch/Lit/Gyal_10_OptiControl2YearsReport.pdf (accessed on 16 January 2017).

19. Gwerder, M.; Gyalistras, D.; Sagerschnig, C.; Smith, R.; Sturzenegger, D. Final Report: Use of Weather and Occupancy Forecasts for Optimal Building Climate Control—Part II: Demonstration (OptiControl-II). Automatic Control Laboratory, ETH Zurich: Zug, Switzerland, 2013. Available online: http://www.opticontrol.ethz.ch/Lit/Gwer_13_Rep-OptiCtrl2FinalRep.pdf (accessed on 16 January 2017).
20. Picard, D.; Sourbron, M.; Jorissen, F.; Vana, Z.; Cigler, J.; Ferkl, L.; Helsen, L. Comparison of Model Predictive Control Performance Using Grey-Box and White-Box Controller Models of a Multi-zone Office Building. In Proceedings of the International Compressor Engineering, Refrigeration and Air Conditioning, and High Performance Buildings Conferences, West Lafayette, IN, USA, 11–14 July 2016.
21. Antonov, S. Short and Long Term Optimal Operation and Robustness Analysis of a Hybrid Ground Coupled Heat Pump System with Model Predictive Control. Ph.D. Thesis, KU Leuven, Leuven, Belgium, July 2016.
22. Killian, M.; Kozek, M. Ten questions concerning model predictive control for energy efficient buildings. *Build. Environ.* **2016**, *105*, 403–412. [CrossRef]
23. De Coninck, R.; Helsen, L. Practical implementation and evaluation of model predictive control for an office building in Brussels. *Energy Build.* **2016**, *111*, 290–298. [CrossRef]
24. Široký, J.; Oldewurtel, F.; Cigler, J.; Prívara, S. Experimental analysis of model predictive control for an energy efficient building heating system. *Appl. Energy* **2011**, *88*, 3079–3087. [CrossRef]
25. West, S.R.; Ward, J.K.; Wall, J. Trial results from a model predictive control and optimisation system for commercial building HVAC. *Energy Build.* **2014**, *72*, 271–279. [CrossRef]
26. Carrascal, E.; Garrido, I.; Garrido, A.J.; Sala, J. Optimization of the heating system use in aged public buildings via model predictive control. *Energies* **2016**, *9*, 251. [CrossRef]
27. Chen, C.; Wang, J.; Heo, Y.; Kishore, S. MPC-based appliance scheduling for residential building energy management controller. *IEEE Trans. Smart Grid* **2013**, *4*, 1401–1410. [CrossRef]
28. Patteeuw, D.; Helsen, L. Combined design and control optimization of residential heating systems in a smart-grid context. *Energy Build.* **2016**, *133*, 640–657. [CrossRef]
29. Kalman, R.E. A new approach to linear filtering and prediction problems. *Trans. ASME J. Basic Eng.* **1960**, *82*, 35–45. [CrossRef]
30. Maasoumy, M.; Razmara, M.; Shahbakhti, M.; Vincentelli, A. Handling model uncertainty in model predictive control for energy efficient buildings. *Energy Build.* **2014**, *77*, 377–392. [CrossRef]
31. Zhang, X.; Schildbach, G.; Sturzenegger, D.; Morari, M. Scenario-based MPC for energy-efficient building climate control under weather and occupancy uncertainty. In Proceedings of the 2013 European Control Conference (ECC), Zürich, Switzerland, 17–19 July 2013.
32. Sturzenegger, D.; Gyalistras, D.; Morari, M.; Smith, R. Model Predictive Climate Control of a Swiss Office Building: Implementation, Results, and Cost–Benefit Analysis. *IEEE Trans. Control Syst. Technol.* **2016**, *24*, 1–12. [CrossRef]
33. Sourbron, M. Dynamic Thermal Behavior of Buildings with Concrete Core Activation. Ph.D. Thesis, KU Leuven, Leuven, Belgium, September 2012.
34. Le, K.; Bourdais, R.; Guéguen, H. From hybrid model predictive control to logical control for shading system: A support vector machine approach. *Energy Build.* **2014**, *84*, 352–359. [CrossRef]
35. Lawal, N.T. An Evaluation of Model Predictive Control of Automated Shading to Optimize. Master's Thesis, Carleton University, Ottawa, ON, Canada, August 2015.
36. Dussault, J.M.; Sourbron, M.; Gosselin, L. Reduced energy consumption and enhanced comfort with smart windows: Comparison between quasi-optimal, predictive and rule-based control strategies. *Energy Build.* **2016**, *127*, 680–691. [CrossRef]
37. Baetens, R.; De Coninck, F.; Jorissen, F.; Picard, D.; Helsen, L.; Saelens, D. OpenIDEAS—An Open Framework for Integrated District Energy Simulations. In Proceedings of the BS2015, 14th Conference of International Building Performance Simulation Association, Hyderabad, India, 7–9 December 2015.
38. Modelica Association. Modelica®—A Unified Object-Oriented Language for Systems Modelling Language Specification. Version 3.3 Revision 1.. 2014. Available online: https://www.modelica.org/ (accessed on 16 January 2017).
39. ASHRAE Inc. *2009 ASHRAE Handbook—FUNDAMENTALS*; ASHRAE: Atlanta, GA, USA, 2009; pp. 10, 31, 176, 300, 305, 312, 313, 319–321.

40. European Committee for Standardization. *EN15251: Indoor Environmental Input Parameters for Design and Assessment of Energy Performance of Buildings Adressing Indoor Air Quality, Thermal Environment, Lighting and Accoustics*; CEN: Brussels, Belgium, 2007; pp. xii, 152, 184, 187, 190, 286, 320, 322.
41. Reynders, G. Quantifying the Impact of Building Design on the Potential of Structural Storage for Active Demand Response in Residential. Ph.D. Thesis, KU Leuven, Leuven, Belgium, September 2015.
42. Awbi, H.B.; Hatton, A. Natural convection from heated room surfaces. *Energy Build.* **1999**, *30*, 233–244. [CrossRef]
43. Olesen, B. Cooling and heating of buildings by activating their thermal mass with embedded hydronic pipe systems. In Proceedings of the ASHRAE-CIBSE, Dublin, Ireland, 3–4 April 2001.
44. Sourbron, M.; Helsen, L. Evaluation of adaptive thermal comfort models in moderate climates and their impact on energy use in office buildings. *Energy Build.* **2011**, *43*, 423–432. [CrossRef]
45. Saelens, D.; Parys, W.; Baetens, R. Energy and comfort performance of thermally activated building systems including occupant behaviour. *Build. Environ.* **2011**, *46*, 835–848. [CrossRef]
46. Li, R.; Yoshidomi, T.; Ooka, R.; Olesen, B. Case-study of thermo active building system in Japanese climate. *Energy Procedia* **2015**, *78*, 2959–2964. [CrossRef]
47. Picard, D.; Jorissen, F.; Helsen, L. Methodology for Obtaining Linear State Space Building Energy Simulation Models. In Proceedings of the 11th International Modelica Conference, Versailles, France, 21–23 September 2015.
48. Safonov, M.G.; Chiang, R.Y. A Schur Method for Balanced Model Reduction. *IEEE Trans. Autom. Control* **1989**, *34*, 729–733. [CrossRef]
49. IBM. CPLEX Optimization Software Package. Available online: http://www-01.ibm.com/software/commerce/optimization/cplex-optimizer/ (accessed on 21 November 2016).
50. Löfberg, J. YALMIP: A Toolbox for Modeling and Optimization in MATLAB. In Proceedings of the CACSD Conference, Taipei, Taiwan, 2–4 September 2004.
51. Freire, R.; Oliveira, G.; Mendes, N. Predictive controllers for thermal comfort optimization and energy savings. *Energy Build.* **2008**, *40*, 1353–1365. [CrossRef]